journal

J. Am. Ceram. Soc., 91 [1] 272–277 (2008)
DOI: 10.1111/j.1551-2916.2007.02142.x

Zirconia Transport by Liquid Convection during Oxidation of Zirconium Diboride–Silicon Carbide

Sigrun N. Karlsdottir† and John W. Halloran

Department of Materials Science and Engineering, University of Michigan, Ann Arbor, Michigan 48104

Anthony Nicholas Grundy

Departement de Genie Chimique Ecole Polytechnique de Montreal, Montreal, Quebec, Canada

During high-temperature oxidation of ZrB_2–SiC composites, a multi-layer oxide scale forms with a silica-rich borosilicate liquid as the surface oxide layer. Here, a recently proposed novel mechanism for the high-temperature oxidation of ZrB_2–SiC composites is further investigated and verified. This mechanism involves the formation of convection cells in the oxide surface layer during high-temperature oxidation of the composite. The formation of zirconia deposits found in the center of the convection cells is proposed here to be the consequence of liquid transport. The nature and deposition mechanism of the zirconia is reported in detail, using calculated phase equilibrium diagrams and microstructure observations of a ZrB_2-15 vol% SiC composite tested at 1550° and 1700°C in ambient air for various times. The calculated phase equilibrium diagrams for the binary ZrO_2–B_2O_3 system as well as the ternary B_2O_3–SiO_2–ZrO_2 system at 1500°C are reported here to interpret these results.

I. Introduction

Composites of zirconium diboride and silicon carbide are prominent members of the class of ultra-high-temperature ceramics (UHTC).[1,2] During high-temperature oxidation of ZrB_2–SiC, a complex multi-layer oxide scale forms,[3,4] featuring some or all of the following features: (1) a silica-rich outer layer, which is believed to act as a protective scale; (2) a subscale of crystalline zirconia, often with a columnar microstructure with silicate between the zirconia grains; and (3) a zirconium diboride region depleted in SiC (the "SiC-depleted region").[5] Relatively little boria is found in the scale. Boria is volatile at oxidation temperatures, so it acts as a transient liquid, presumably evaporating from the external surface. The mechanism of formation of this complex scale is of interest, and this paper addresses this issue from the perspective of zirconia transport.

Recently, we reported[6] the formation of distinct flower-shaped convection cells in the silica-rich outer layer. These convection cells transported boria-rich liquid to the surface, where it apparently evaporated. Zirconium oxide (ZrO_2) was found in the center of the convection cells, leading to a pattern of ZrO_2 decorating the surface. This paper reports in detail the nature and deposition mechanism of this zirconia, using microstructure observations and calculated phase equilibrium diagrams.

A. Zangvil—contributing editor

Manuscript No. 23021. Received April 2, 2007; approved September 20, 2007.
This work was supported by the Office of Naval Research (USA), under Grant No. N 0014-02-1-0034.
†Author to whom correspondence should be addressed. e-mail: nanna@umich.edu

II. Experimental Methods

(1) Fabrication and Oxidation Testing

The material was a hot pressed ZrB_2–15-vol% SiC ceramic fabricated at ISTEC-CNR (The Institute of Science and Technology for Ceramics, National Research Council, Faenza, Italy). Properties and processing are presented in more detail elsewhere.[7] A ball-milled powder mixture was uniaxially hot-pressed at 1820°C for 15 min at 30 MPa applied pressure. The tested specimens were rectangular cuboids with an average total surface area of 1 cm^2. Oxidation was conducted in ambient laboratory air either by heating specimens to 1550°C with a heating rate of 13°C/min and free cooling in a conventional furnace (Lindberg, Watertown, WI), or by the use of a novel ribbon apparatus, described in detail elsewhere.[8] Briefly, the ribbon apparatus used self-supported ribbon samples,[7] which were self-heated by electrical resistance. In the conventional furnace, the specimens were supported on pieces of the same material, and heated in stagnant ambient air. Specimens were ultrasonically cleaned in acetone and dried before oxidation. After oxidation, specimens were stored in moisture-free desiccators to avoid any reaction of a B_2O_3 on the surface of the specimens. Cross-section of the oxidized specimen was prepared for microstructural analysis by nonaqueous polishing procedures down to 0.5-μm finish. The composition and morphology of the oxide scales were characterized by scanning electron microscopy (SEM), backscattering electron microscopy (BSE), and X-ray energy dispersive spectroscopy (XEDS) using a Philips XL30 FEG SEM (Amsterdam, the Netherlands). A Cameca SX100 (Trumbull, CT) was used for electron microprobe analysis (EMPA), using well-characterized mineral standards for quantitative analysis of boron, zirconium, and silicon, and for imaging in the BSE and cathodoluminscence (CL) modes.

III. Equilibrium Phase Diagram Calculations

The phase diagrams of the ternary SiO_2–B_2O_3–ZrO_2 system were calculated using the commercial FactSage software package. The thermodynamic properties of all solid phases are taken from the FT-Oxide database.[9] The ternary liquid phase was calculated using the modified quasichemical model.[10] The thermodynamic description of the liquid phase of the SiO_2–B_2O_3 is taken from Decterov *et al.*[11] The SiO_2–ZrO_2 system was optimized based on the experimental phase diagram by Butterman and Foster.[12,13] These authors give the eutectic, monotectic, and critical points of the miscibility gap at 1687°, 2250°, and 2430°C, respectively. By introducing two temperature-independent positive interaction parameters, these temperatures can be reproduced within experimental accuracy giving 1688°, 2252°, and 2388°C, respectively. The B_2O_3–ZrO_2 binary system was optimized based on the experimental investigations by Beard *et al.*[14] These authors give the ZrO_2 solubility as 0.9 mol% at 1200°C and state that optical examination of the glass in

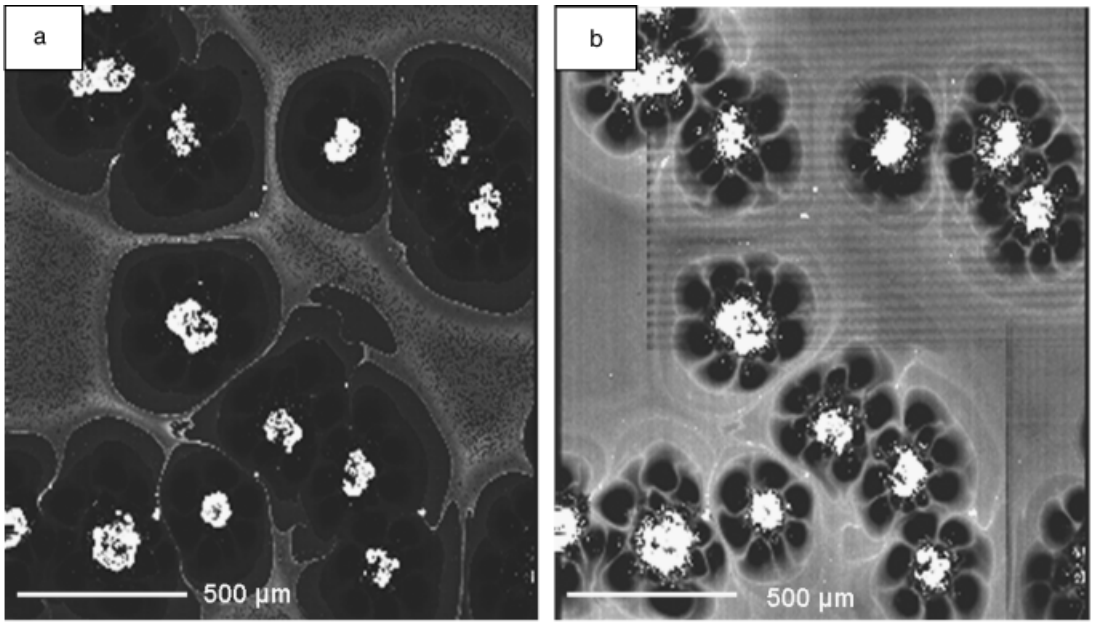

Fig. 1. Surface of a ZrB_2–15 vol% SiC sample oxidized for 2 h at 1550°C. (a) Back-scattered electron image showing zirconia in bright contrast; (b) same area imaged by cathodoluminesence showing petal-like lobes in dark contrast.

compositions ranging from 88 mol% B_2O_3–12 mol% ZrO_2 to 97 mol% B_2O_3–3 mol% ZrO_2 heated between 900° and 1400°C indicated liquid–liquid immiscibility. We optimized a single positive interaction parameter for this binary system in order to reproduce the experimental ZrO_2 solubility at 1200°C. The calculated ZrO_2–B_2O_3 phase diagram is shown in Fig. 10. The optimized phase diagram indicates a metastable miscibility gap in the B_2O_3-rich region, shown as a dotted line with a critical temperature of 1062°C, which could account for the liquid–liquid immiscibility observed by Beard *et al.*[14] The liquidus of the ternary system is predicted by symmetrically extrapolating[10] the binary interaction parameters to the ternary system. An isothermal section of the ternary ZrO_2–SiO_2–B_2O_3 phase diagram, calculated at 1500°C, is shown in Fig. 9. Because of the scarcity of experimental data the calculated phase diagrams must be regarded as somewhat speculative. However, the general features of the system can be expected to be qualitatively correct. This ternary system is very interesting from a thermodynamic point of view, as all three bordering binary systems show either stable (system ZrO_2–SiO_2) or metastable (systems SiO_2–B_2O_3 and ZrO_2–B_2O_3) liquid–liquid miscibility gaps. Hopefully, future experimental investigations will shed more light on this system.

IV. Results and Discussion

Figure 1 shows the surface of the oxide film on a sample oxidized for 120 min at 1550°C in a conventional furnace, sufficient to grow an oxide with about 40 μm of zirconia covered with about 20 μm of silica-rich glass. On the left in Fig. 1(a) is an image taken with backscattered electrons showing the notable "island-in-lagoon" features, where approximately 100-μm islands in bright contrast are surrounded by approximately 500-μm diameter "lagoons" in darker contrast. Note that the width of these features is several times larger than the oxide-scale thickness. These features are separated by areas in lighter gray contrast. The bright island features are shown by XEDS to

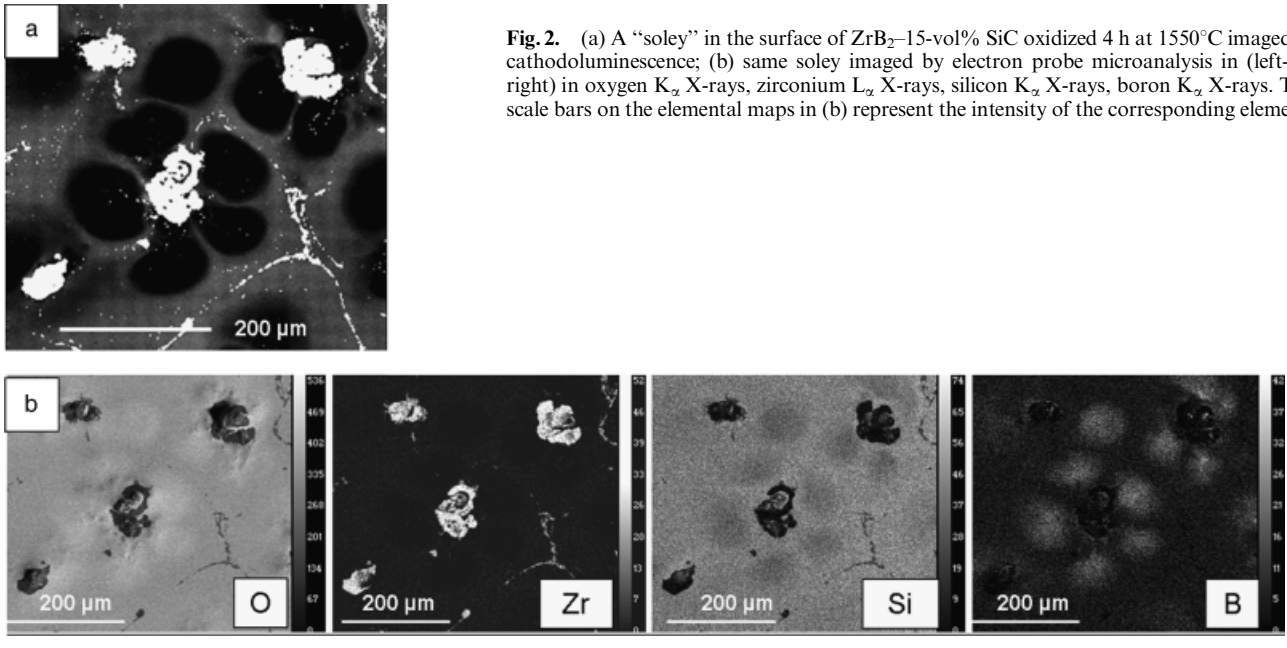

Fig. 2. (a) A "soley" in the surface of ZrB_2–15-vol% SiC oxidized 4 h at 1550°C imaged in cathodoluminescence; (b) same soley imaged by electron probe microanalysis in (left-to-right) in oxygen K_α X-rays, zirconium L_α X-rays, silicon K_α X-rays, boron K_α X-rays. The scale bars on the elemental maps in (b) represent the intensity of the corresponding element.

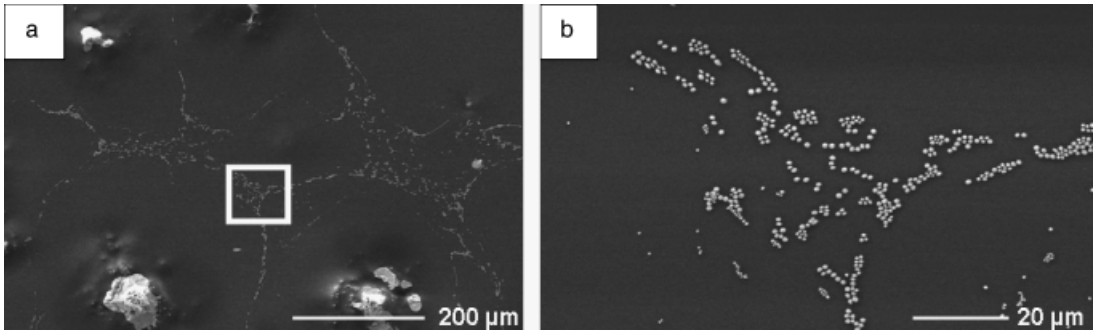

Fig. 3. Surface of specimen oxidized at 1550°C for 4 hours showing features suggesting flow along the surface. (a) Shows several lagoon-like features; note the apparent flow patterns of the fine zirconia particles between lagoons. (b) Higher magnification of the small zirconia particles between the lagoon-like features highlighted by the white box in Fig. 3(a).

consist of zirconia, while the darker lagoon features are primarily silica. The lighter gray regions consist of silica decorated with many approximately 1-μm zirconia particles. The same area imaged by CL is presented in Fig. 1(b) on the right. The CL image reveals a flower-like pattern inside the lagoon features, with petal-like lobes in dark CL contrast surrounding the central zirconia island. These flower patterns resemble the Islandic soley *Ranuculus acris*, or common Buttercup, so we will refer to them as soleys. Figure 2 shows a soley feature in a sample oxidized at 1550°C for 4 h, imaged in CL and by X-rays excited from oxygen (O), zirconium (Zr), silicon (Si), and boron (B). This confirms that the lobes in dark contrast in CL are rich in boria but relatively poor in silica, and that the central island feature is zirconia containing little silica. Elsewhere[6] we have argued that soleys are convection cells that transport a fluid boria–silica–zirconia oxide (BSZ) liquid to the surface, where it flows laterally, creating the lagoon features. Evaporation of the volatile boria from the soley pedals at the surface deposits viscous silica liquid, forming the lagoon features, and solid zirconia, forming the island features.

Zirconia is also present on the surface as discrete particles, about 1 μm in diameter. These are shown in Fig. 3, where we see that the small zirconia particles are not seen inside the lagoon features, but rather between them. Notice the pattern of small particles between the lagoon features in Fig. 3(a), which seem to define flow patterns. The fine scale arrangement of the particles (Fig. 3(b)), also suggests particles moved by a flowing liquid. These fine zirconia particles can also be seen inside the glassy silica layer, often arranged in horizontal layers. An example is shown in Fig. 4, a fracture surface of the cross section of the glassy scale. Note the repeated layers of fine zirconia particles separated by thin layers of particle-free silica glass. We suggest that these layers of zirconia particles were once decorating the surface (as in Fig. 3), but were subsequently covered by silica-rich liquid, and this process was repeated several times. The thickness of the particle-free silica layers varies from about 5 μm near the bottom of the scale to about 2 μm near the middle of the scale, which might suggest that the extent of the lateral flow of liquid changes with oxidation time.

In Fig. 5 we present a fractured cross section of ZrB_2–15-vol% SiC specimen oxidized for 15 min at 1700°C in the ribbon apparatus, showing (from the interior) unoxidized ZrB_2–SiC interior, an SiC-depleted zone of ZrB_2, a layer with columnar zirconia, and an outer glassy layer. The surface of the sample shows many protuberances, which consist of a core of zirconia surrounded by glass. The central zirconia "islands" (imaged from the top in Figs. 1 and 2) are shown to be protuberances elevated 5–10 μm above the silicate glass surface. We suggest that the protuberances are associated with the convection cells.

The samples are rectangular cuboids. During oxidation the top surface (y–z plane) is horizontal while the side surface (x–z plane) is vertical. Figure 6 shows a corner of a ZrB_2–SiC composite oxidized for 4 h at 1550°C in a conventional furnace. The horizontal top (y–z) surface is on the left, with the vertical (x–z) side surface to the right. Convection cells decorate the side and top surface of the specimen. Note that the structure is similar on the top and side, demonstrating that the direction of gravity does not influence the shape of convection features. This suggests that the convection is not driven by density difference (due to thermal gradient), for if it were density driven the shape of the features would be different on the top and side, or normal to and perpendicular to the gravity vector. Elsewhere[6] we suggested that convection is mechanically driven by the large molar volume increase due to oxidation. Figure 7 is an image taken with backscattered electrons showing a cross-sectional view of one of the zirconia islands precipitated from the BSZ

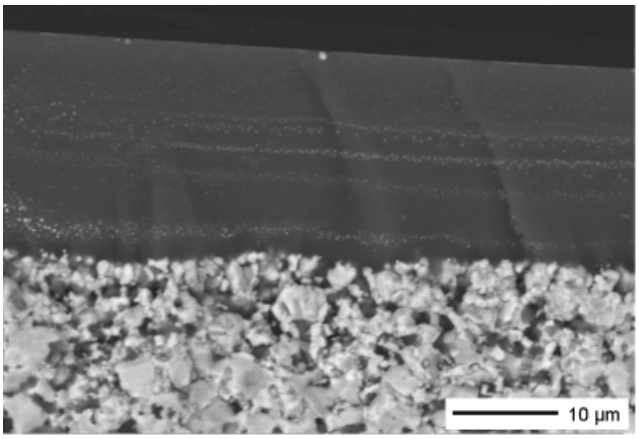

Fig. 4. Fracture surface cross-section of sample showing strata of small zirconia particles, suggesting layers of fine surface particles (as in Fig. 3) repeatedly covered by liquid.

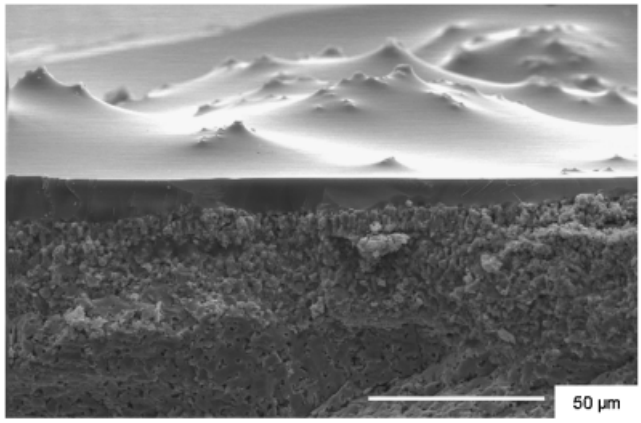

Fig. 5. Fractured cross-section of ZrB_2–15-vol% SiC specimen oxidized for 15 min at 1700°C in the ribbon apparatus showing (from the interior): the unoxidized interior, the SiC-depleted zone, a columnar zirconia layer, and outer glassy layer.

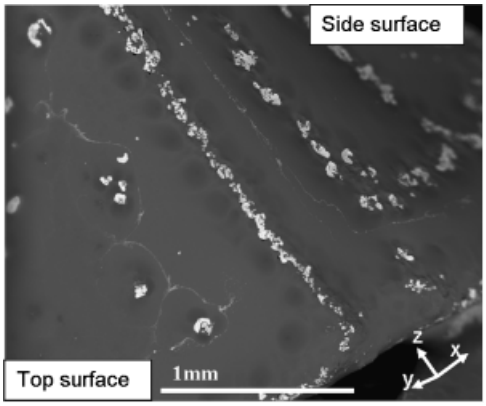

Fig. 6. Corner of the surface of a ZrB_2–SiC composite oxidized for 4 h at 1550°C in a conventional furnace. Convection cells decorate the side surface (x–z) and top surface (y–z) of the specimen. Note that the structure is similar on top and side, demonstrating that the direction of gravity does not affect shape of the convection features.

liquid when the boria was lost by evaporation. The remaining BS liquid flowed over the surface until enough boria had evaporated to leave only remnant silica.

Details of the growth of the protuberances might be also inferred from Fig. 8, which is a fracture surface of the sample oxidized at 1700°C for 15 min in the ribbon apparatus. Here the fracture plane has intersected two zirconia protuberances. The summits of both protuberances are decorated with fine zirconia particles. Beneath the protuberances are what appear to be columns of discrete zirconia particles in a glassy matrix. Figure 8(b) is a higher magnification of the columns of the zirconia particles, showing the structure in details. We suggest that each of these zirconia particles was formed when the ZrO_2 dissolved in the BSZ liquid precipitated at the surface. Subsequently the zirconia particles were buried by fresh deposits from BSZ liquid, which continued to be transported to the surface by the convection cells.

The existence of a BSZ liquid is essential for the proposed convection mechanism of zirconia transport. The system B_2O_3–SiO_2 is known to form liquid solutions, but experimental data for the solubility of ZrO_2 in B_2O_3–SiO_2 liquids have not been reported. The only published report of phase equilibrium in the B_2O_3–SiO_2–ZrO_2 system is by Butterman,[13] but his emphasis was on the geological conditions for zircon formation. Consequently we use computational thermochemistry to predict the behavior of the B_2O_3–SiO_2–ZrO_2 system. Figure 9 is a calculated phase diagram for the isothermal section of the B_2O_3–SiO_2–ZrO_2 system at 1500°C, showing equilibrium between a BSZ liquid solution (liquid) and crystalline phases of zirconia (ZrO_2), zircon ($ZrSiO_4$), and silica (SiO_2). We will make use of this phase diagram to interpret the phase behavior and microstructure of the oxides in the following section. The solubility of zirconia in a boron oxide (B_2O_3) liquid for the binary system ZrO_2–B_2O_3 is shown in Fig. 10. Notice that a transient B_2O_3 liquid can dissolve much more zirconia at higher temperatures. The mole fraction zirconia, X_{ZrO_2}, in the zirconia-saturated liquid at 1550°C is about 0.2 in the binary, but at 1800°C the boron oxide liquid can dissolve up to 37-mol% zirconia. This suggests that a transient boron oxide liquid would be a more potent transport medium for zirconia at higher temperatures, at least for conditions below the boiling point of boron oxide (about 2200°C in air). Agents that promote boron oxide vaporization, such as water,[15] decrease the temperature range where boron oxide liquids can exist, and should retard transport of dissolved zirconia and silica by the transient boron oxide-rich liquid.

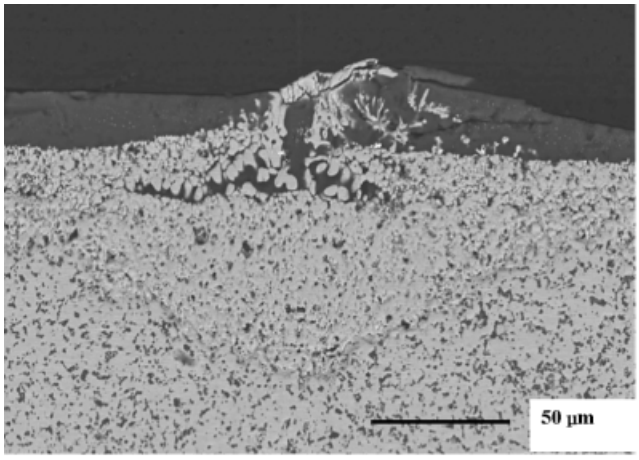

Fig. 7. Backscattering electron microscopic image of the cross-section of a ZrB_2–SiC specimen tested at 1550°C for 4 h in a conventional furnace. The image shows a zirconia island along with some secondary zirconia surfacing the oxide boria–silica–zirconia liquid.

(1) Analysis of Oxide Scale Microstructure Development

Some assumptions are necessary to estimate the composition and amounts of the phases produced by oxidation. It appears that relative thickness of the SiC-depleted zone and thickness of the zirconia layer does not change much with time. This suggests that the diboride and the SiC oxidize in the same ratio as they are present (no marked preferred oxidation). This implies that in the ratio expected for oxidation of 85-vol% ZrB_2–15-vol% SiC (or 79-mol% ZrB_2), the composition of fresh liquid oxide should have a boron to silica ratio $X_{B_2O_3} : X_{SiO_2}$ of 0.79:0.21. Solid zirconia is also produced, and some of this will dissolve in the liquid. According to the calculated phase diagram, a zirconia-saturated borosilicate (BSZ liquid) with this B/Si ratio dissolves about 11 mol%.

We expect the phase assemblage for the complete oxidation of ZrB_2–15-vol% SiC at 1500°C to be, on a molar basis, 0.33 mole solid ZrO_2 and 0.67 moles of a BSZ liquid (liquid composition 71-mol% Boria+18-mol% silica+11-mol% zirconia). We presume that the solid undissolved zirconia remains at the interface with ZrB_2 as the "primary zirconia," while the BSZ liquid flows out to the surface, carrying dissolved zirconia. The BSZ liquid can transport the dissolved zirconia to another location, where it might precipitate as zircon or as "secondary" zirconia.

Boria and, to a lesser extent, silica can evaporate from the BSZ liquid at the external surface, changing the composition of the remaining liquid. Boron oxide is much more volatile, with a vapor pressure of 233 Pa at 1500°C.[5] The vapor pressure of silica is only 3×10^{-4} Pa at 1500°C.[16] At the surface, essentially all of the boria will evaporate. Depending on the temperature and atmosphere, some of the silica might also evaporate, but none of the zirconia will be removed by evaporation. Consider the case where only the boria is volatile. As the boria evaporates, the remaining liquid moves into the two-phase region liquid+solid ZrO_2, as defined by the tie lines in the phase diagram. As boria is evaporated, the remaining BSZ liquid becomes richer in silica, and zirconia must precipitate from the BSZ liquid. Thus we expect the formation of secondary zirconia precipitates, located near the site of boria evaporation. The secondary zirconia will be precipitated from a liquid, and might have a different morphology from the primary zirconia, suggesting that it might be possible to distinguish secondary zirconia within the microstructure. The zirconia precipitates will either remain at the location where they formed, or be carried as a dispersed particle with the flowing BSZ liquid.

We expect the viscosity of the BSZ liquid to change dramatically as the fluid boria component is lost and the remaining BSZ is enriched in silica. Very little data are available for the viscosity of borosilicate liquids (and no data exist for zirconia-containing borosilicate). However, we can consider the known values for the 1550°C viscosity of silica ($\eta_{SiO_2} = 100$ GPa·s) and boria ($\eta_{B_2O_3} = 40$ Pa·s), combined with a viscosity for one interme-

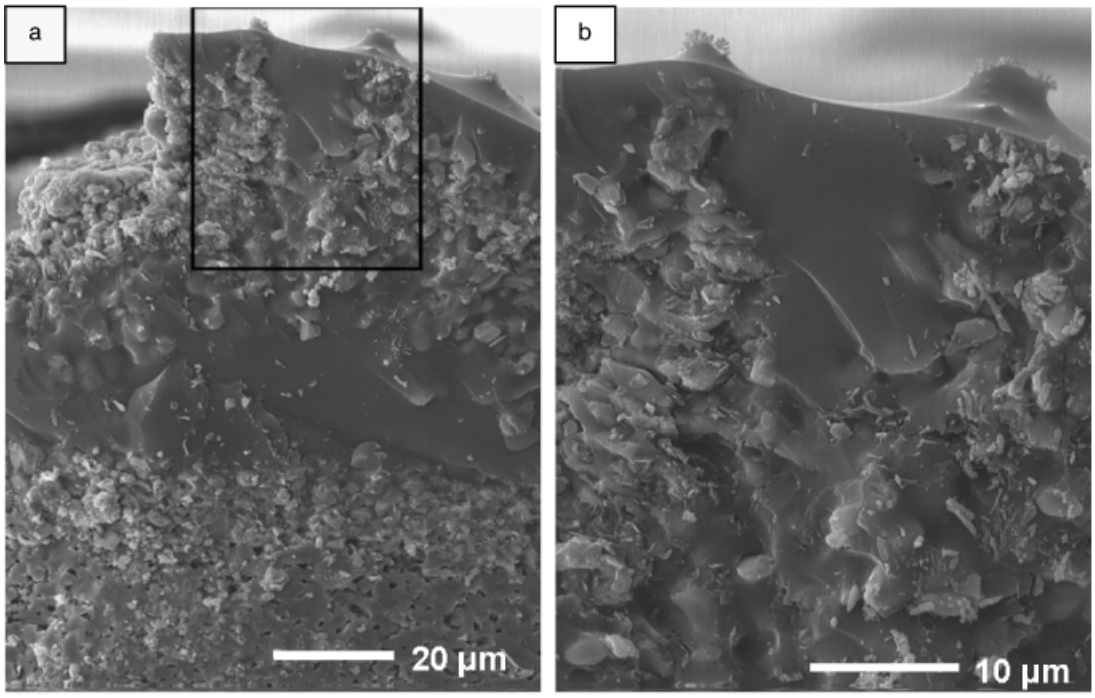

Fig. 8. (a) Fracture surface of a ZrB_2–SiC oxidized at 1700°C for 15 min in the ribbon apparatus, where the fracture plane has intersected two zirconia peaks. (b) A higher magnification of the area highlighted with the white box in (a) showing the details of the zirconia peaks. Note their appearance as columns of discrete zirconia particles in a glassy matrix.

diate composition[17] to obtain a rough estimate for the change in the viscosity of the borosilicate (η_{BS}) with mole fraction boria ($X_{B_2O_3}$), which is approximately

$$\log_{10}\ \eta_{BS} = 11 - 9X_{B_2O_3} \quad (1)$$

For a 85-vol% ZrB_2–15-vol% SiC composite, the composition of the fresh liquid oxide should have a boron to silica ratio $X_{B_2O_3} : X_{SiO_2}$ of 0.79:0.21; thus the viscosity of the boron oxide-rich liquid can be roughly estimated to be around $\eta_{SiO_2-B_2O_3} \sim 1000$ Pa · s. Eventually, as approximately 95% of the boria has evaporated, the viscosity of the remaining liquid (η_{BS}) has increased to the order of 10 GPa · s.

If boron oxide would completely evaporate from the transient BSZ liquid of composition 71-mol% boria+18-mol% silica +11-mol% zirconia, we would move into the two-phase region where zircon ($ZrSiO_4$) precipitates and the final equilibrium phase assemblage would be a two-phase mixture, zircon and solid SiO_2, in the ratio of about 75-mol% zircon–25-mol% SiO_2. (We observe zirconia, not zircon, but $ZrSiO_4$ is not very stable at these temperatures, so perhaps it does not form.) Assuming that evaporation of boron stops due to the increase in viscosity of the liquid when about 10-mol% B_2O_3 remains in the liquid, the total composition moves to 58-mol% SiO_2, 36-mol% ZrO_2, and 6-mol% B_2O_3. The equilibrium phase assemblage at this composition is 66 mol% of a silica-rich liquid and 34-mol% solid zirconia. The microstructure of the zirconia will be different as it is secondary zirconia precipitated from the liquid following boron evaporation. These considerations are in reasonable agreement with the observed volume fractions, estimated by stereological analysis of the glassy layer, which suggests about 75 vol% (~70 mol%) silica and about 25 vol% (~30 mol%) precipitated zirconia (as distinct from the columnar zirconia).

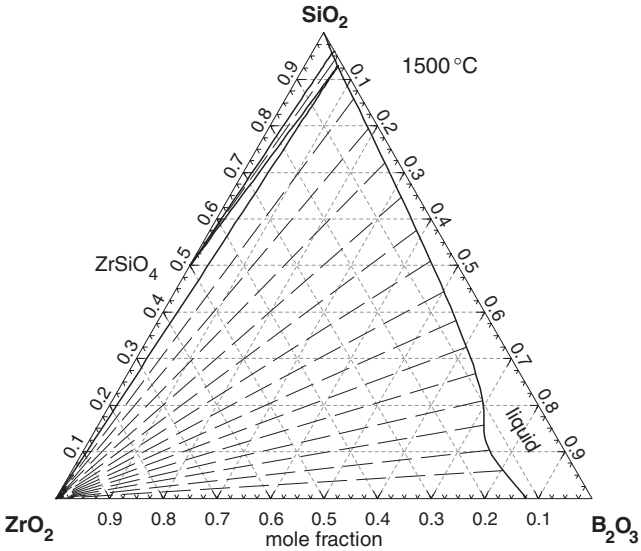

Fig. 9. Calculated phase diagram for the 1500°C isothermal section of the ternary ZrO_2–SiO_2–B_2O_3, showing equilibrium between a boria–silica–zirconia liquid and crystalline phases of ZrO_2, $ZrSiO_4$, and SiO_2.

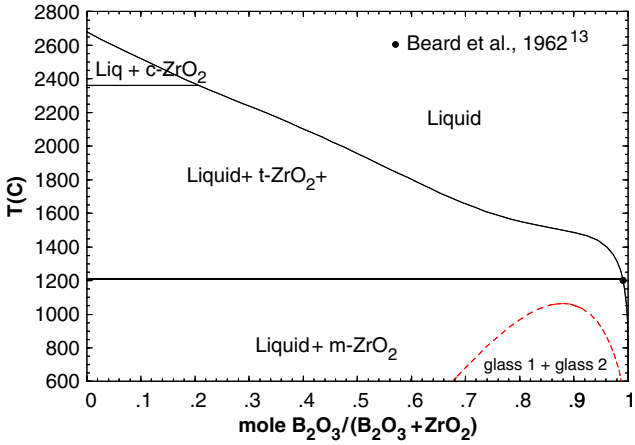

Fig. 10. Calculated binary phase diagram for the system ZrO_2–B_2O_3, showing the solubility of zirconia in the boron oxide liquid as a function of temperature.

(2) Speculations on the Oxidation of ZrB_2

It is tempting to examine the microstructure of the zirconia oxide layer that forms on pure zirconium diboride without additives. Presumably this oxide forms crystalline zirconia and a transient BZ liquid:

$$ZrB_2 + 5/2\ O_2 = (1-x)(ZrO_2)_{\text{crystalline}} + (B_2O_3 + x\ ZrO_2)_{\text{liquid}} \quad (2)$$

At 1500°C, the binary phase diagram suggests that the mole fraction of primary zirconia is about 0.43 of the total composition, and the amount of the (B_2O_3+ZrO_2) liquid is about 0.57. The (B_2O_3+ZrO_2) liquid has a composition of 13-mol% dissolved zirconia and 87-mol% B_2O_3. If all the B_2O_3 evaporates away, the primary zirconia would be 85-mol% and the precipitated secondary zirconia 15-mol% of the total solid zirconia. Fahrenholtz[16] presents a micrograph of a specimen of zirconium diboride oxidized in air at 1500°C for 30 min, with about a 63-μm surface layer of porous zirconia. This particular micrograph appears to have two distinct morphologies of zirconia grains: inner grains of the order of 5–6 μm in size, perhaps with a columnar structure, and smaller grains, 1–2 μm, perhaps more equiaxed, located closer to the external surface. It appears that the fine-grained outer zirconia layer is about 10-μm thick, while the large-grained inner layer is about 53-μm thick. This is about the proportion one might expect if the inner grains were primary zirconia (at ~85% of the total zirconia) while the outer grains were secondary zirconia deposited after evaporation of the boron oxide solvent. This suggests that transient liquid BZ solution might influence the microstructure of the porous zirconia scales on ZrB_2 even in the absence of silica from SiC.

V. Conclusions

The formation of zirconium oxide found in the center of convection cells, introduced in a previous article by the authors,[6] during high-temperature oxidation of ZrB_2–SiC composites, is proposed here to be the consequence of liquid transport. A fluid BSZ liquid is transported to the surface through the convection cells due to a larger volume increase produced when the ZrB_2–SiC material oxidizes at high temperatures, proposed in a previous article by the authors. There, the BSZ liquid flows laterally, creating convection patterns when the boria (B_2O_3) evaporates. Here we propose that the ZrO_2 in the center of the cells forms when it starts precipitating from the BSZ liquid during B_2O_3 evaporation. When ZrO_2 precipitates, the liquid becomes mainly viscous silica (SiO_2) liquid, which flows outward. These conclusions are based on chemical and microstructural observations as well as on phase behavior predicted by calculated binary ZrO_2–B_2O_3 and ternary B_2O_3–SiO_2–ZrO_2 phase equilibrium diagrams. The calculated phase diagrams are reported here for the first time. The existence of a BSZ liquid is essential for the proposed convection mechanism of zirconia transport. The calculated phase diagram for the isothermal section of the B_2O_3–SiO_2–ZrO_2 system at 1500°C shows equilibrium between a BSZ liquid solution (liquid) and crystalline phases of zirconia (ZrO_2), zircon ($ZrSiO_4$), and silica (SiO_2). For a ZrB_2–15 vol% SiC composite (79-mol% ZrB_2–21-mol% SiC) we assume that the composition of the fresh liquid oxide with a B_2O_3 to SiO_2 ratio, $X_{B_2O_3} : X_{SiO_2}$, is 0.79:0.21. For that ratio the maximum solubility of ZrO_2 in the BSZ liquid is 11 mol%, predicted from the ternary phase diagram. When the B_2O_3 starts to evaporate from the BSZ liquid it moves into the two-phase region with solid ZrO_2 and BSZ liquid. The remaining BSZ liquid then becomes richer in silica as the boria continuous to evaporate, and zirconia precipitates from the BSZ liquid. Thus the formation of secondary zirconia located near the site of boria evaporation is expected. From microstructure analysis of the surface of the specimen the secondary zirconia precipitates can either remain at the location where they formed or be carried as dispersed particles by the flowing liquid, where they serve as remnant markers of the flow pattern after the liquid cools to the SiO_2-rich glass.

These findings support and expand a novel mechanism of high-temperature oxidation of ZrB_2–SiC material, based on liquid flow and formation of convection cells, proposed in a previous article by the authors.[6]

Acknowledgments

S. N. K. and J. W. H. thank Carl Henderson from the EMAL for his vital assistance with characterization, particularly CL. We thank Alida Bellosi and her associates of ISTEC in Faenza, Italy, for providing the materials.

References

[1]S. R. Levine, E. J. Opila, M. C. Halbig, J. D. Kiser, M. Singh, and J. A. Salem, "Evaluation of Ultra-High Temperature Ceramics for Aeropropulsion Use," *J. Eur. Ceram. Soc.*, **22**, 2757–67 (2002).

[2]M. M. Opeka, I. G. Talmy, and J. A. Zaykoski, "Oxidation-Based Materials Selection for 2000°C+Hypersonic Aerosurface: Theoretical Considerations and Historical Experience," *J. Mater. Sci.*, **39** [19] 5887–904 (2004).

[3]F. Monteverde and A. Bellosi, "Oxidation of ZrB_2-Based Ceramics in Dry Air," *J. Electrochem. Soc.*, **150** [11] B552–9 (2003).

[4]E. J. Opila, S. R. Levine, and J. Lorincz, "Oxidation of ZrB_2- and HfB_2-based Ultra-High Temperature Ceramics: Effect of Ta Additions," *J. Mater. Sci.*, **39**, 5969–77 (2004).

[5]W. G. Fahrenholtz, "Thermodynamics of ZrB_2–SiC Oxidation: The Formation of a SiC-Depleted Region," *J. Am. Ceram. Soc.*, **90** [1] 143–8 (2007).

[6]S. N. Karlsdottir, J. W. Halloran, and C. E. Henderson, "Convection Patterns in Liquid Oxide Films on Zirconium Diboride–Silicon Carbide Composites Oxidized at High Temperature," *J. Am. Ceram. Soc.*, **90** [9] 2863–7 (2007).

[7]S. N. Karlsdottir, J. W. Halloran, F. Monteverde, and A. Bellosi "Oxidation of ZrB_2–SiC: Comparison of Furnace Heated Coupons and Self-Heated Ribbon Specimens," *Proceedings of the International Conference on Advanced Ceramics and Composites*, Daytona Beach, FL, January 21–26, 2007 (accepted, May 2007).

[8]S. N. Karlsdottir and J. W. Halloran, "Rapid Oxidation Characterization of Ultra-High Temperature Ceramics," *J. Am. Ceram. Soc.*, **90** [10] 3233–8 (2007).

[9]C. W. Bale, P. Chartrand, S. A. Degterov, G. Eriksson, K. Hack, R. Ben Mahfoud, J. Melanqon, A. D. Pelton, and S. Petersen, "FactSage Thermochemical Software and Databases," *Calphad*, **26** [2] 189–228 (2002). Available at http://www.factsage.com.

[10]A. D. Pelton and M. Blander, "Thermodynamic Analysis of Ordered Liquid Solutions by a Modified Quasichemical Approach—Application to Silicate Slags," *Metal. Trans. B*, **17B**, 805–15 (1986).

[11]S. A. Decterov, V. Swami, and I.-H. Jung, "Thermodynamic Modeling of the B_2O_3, B_2O_3–SiO_2 and the B_2O_3–Al_2O_3 Systems," *Int. J. Mater. Res.*, accepted.

[12]W. C. Butterman and W. R. Foster, "Zircon Stability and the Zirconium Oxide-Silica Phase Diagram," *Am. Mineral.*, **52** [5-6] 880–5 (1967).

[13]W. C. Butterman, "Equilibrium Phase Relations among Oxides in the Systems GeO_2, GeO_2–B_2O_3, HfO_2–B_2O_3, ZrO_2–SiO_2–B_2O_3, and ZrO_2–SiO_2," Ph.D. Dissertation, Ohio State University, Columbus, OH, 1965.

[14]W. C. Beard, W. C. Butterman, D. E. Koopman, H. E. Wenden, and W. R. Foster "Research on Phase Equilibria between Boron Oxides and Refractory Oxides, Including Silicon and Aluminum Oxides," Quarterly Progress Report No. 9, October 1, 1961–December 31, 1961, Technical Report, Ohio State University Research Foundation, Columbus, OH, January 15, 1962.

[15]Q. N. Nguyen, E. J. Opila, and R. C. Robinson, "Oxidation of Ultra High Temperature Ceramics in Water Vapor," NASA/TM-2004-212923, April 2004.

[16]W. G. Fahrenholtz, "The ZrB_2 Volatility Diagram," *J. Am. Ceram. Soc.*, **88** [12] 3509–12 (2005).

[17]R. Jabra, J. Phalippau, and J. Zarzicki, "Synthesis of Binary Glass-Forming Oxide Glasses by Hot-Pressing," *J. Non-crystalline Solids*, **42**, 489–98 (1980). □